



Effects of Temperatures on Strength and Deformability of Tak Granite

*Kittikron Rodklang, Supattra Khamrat and Kittitep Fuenkajorn**

Geomechanics Research Unit, Suranaree University of Technology, 111 University Avenue, Nakhon Ratchasima 30000, Thailand

**Correspondent author: kittitep@sut.ac.th*

Abstract

Strength of granite under elevated temperatures is an important parameter governing the long-term stability of waste disposal boreholes. The objective of this study is to experimentally determine the effects of elevated temperatures on the compressive strengths and elasticity of Tak granite. The rock strength and deformability are determined under various temperatures and confining pressures. The confining stresses are maintained constant at 0, 3, 7, to 12 MPa using a polyaxial load frame. The rectangular block specimens have nominal dimensions of $5 \times 5 \times 10 \text{ cm}^3$. The testing temperatures are varied from 273 to 773 Kelvin. The results indicate that the granite strength and elasticity exponentially decrease as the temperature increases. The distortional strain energy criterion is proposed to describe the rock strengths as a function of mean strain energy. The criterion fits well to the test results. The proposed strength criterion is useful to predict the strength and deformation of granite around waste disposal boreholes under elevated temperatures.

Keywords: *strain energy, elevated temperature, strength, elasticity*

1. Introduction

The effects of temperature on deformability and strength of rocks have long been recognized (1, 2). A number of new topics have been raised, related to rock mechanics, given an increasing demand for underground storage of nuclear waste, natural gas and petroleum, as the rate of exploration for energy resources on a worldwide scale accelerates (3). The rock temperature around the nuclear waste in such conventional storage may not rise beyond 523 K

(4, 5). But, in the case of non-conventional or direct burial of nuclear waste the rock temperature may be very high and sometimes exceeds the melting point of the rock (6, 7). The mechanical behavior of rocks essentially depends upon mineralogy, structure, temperature, stress and time (8). The knowledge of thermo-mechanical behavior of rock is imperative because high temperature leads to development of new micro-cracks or extension/widening of pre-existing micro-cracks within the rocks.

This phenomenon affects the strength of rocks (9).

The objective of this study is to develop a multi-axial strength criterion for granite under various temperatures and confining pressures. The criterion will be useful to assess the mechanical stability of the granite around borehole under elevated temperature. The predictability of the proposed criterion is verified by the results of uniaxial and triaxial compressive strength and Brazilian tensile strength tests on granite specimens tested under nominal temperatures of 273, 303, 373, 573 and 773 K.

2. Granite Specimens

The rock samples used in this research is obtained from Tak Batholiths, western Thailand. The granite shows an extended compositional range, calc-alkaline, rich accessory minerals and K-feldspar (10). The specimens have been prepared to obtain rectangular blocks with nominal dimensions of $5 \times 5 \times 10 \text{ cm}^3$ for the uniaxial and triaxial compression tests that comply with the ASTM D-4543-85 (11). A total of 20 specimens are prepared for each temperature level. The Brazilian tension test uses disk specimens with a nominal diameter of 5.4 cm with a thickness-to-diameter ratio of 0.5 to comply with ASTM D 3967-95 (12). The thermal properties of the Tak granite determined here are as follows: thermal diffusivity = $1.71 \pm 0.04 \text{ mm}^2/\text{s}$, thermal conductivity = $2.22 \pm 0.01 \text{ W/mK}$, specific heat = $1.30 \pm 0.03 \text{ MJ/m}^3\text{K}$ and thermal expansion = $1.8 \times 10^{-7} \text{ K}^{-1}$.

3. Test Method

The uniaxial and triaxial compression tests are performed to determine the compressive strength and deformation of granite specimen under various confining

pressures and temperatures. A polyaxial load frame (13) has been used to apply axial and lateral stresses to the granite specimens (Figure 1). The test frame utilizes two pairs of cantilever beams to apply lateral stresses to the specimen while the axial stress is applied by a hydraulic cylinder connected to an electric pump. The uniform lateral stresses on the specimens range from 0, 3, 7 to 12 MPa, and the constant axial stress rate of 1 MPa/s is applied until failure occurs. The specimen deformation monitored in the three principal directions is used to calculate the principal strains during loading. The failure stresses are recorded and mode of failure examined. The load frame has an advantage over the conventional triaxial (Hoek) cell because it allows a relatively quick installation of the test specimen under triaxial condition, and hence the change or deviation of the specimen temperature during testing is minimal.

The Brazilian tensile strength of the granite has been determined from disk specimens with temperatures ranging from 273, 303, 373, 573 to 773 K, with the constant axial stress rate of 1 MPa/s. except the pre-heating and cooling process, the test procedure, sample preparation and strength calculation follow the ASTM D 3967-08 (14). The tests are performed by applying diametrical line load to the rock disk specimen until failure occurs.

Steel platens with heater coil are the key component for this experiment. They are incorporated into the polyaxial load frame (Figure 1). Electric heating is through a resistor converts electrical energy into heat energy. Electric heating devices use Nichrome (Nickel-Chromium Alloy) wire supported by heat resistant. A thermostat is a component of a control system which

senses the temperature of a system so that the system's temperature is maintained near a desired set point. A heating element converts electricity into heat through the process of resistive. Electric current passing through the element encounters resistance, resulting in heating of the element. The thermostat is SHIMAX MAC5D-MCF-EN Series DIGITAL CONTROLLER. The digital controller is 48×48 mm with panel depth of 62-65 mm. Power supply is a 100-240V ± 10%AC on security surveillance system. The accuracy is ± 0.3%FS + 1digit. The thermocouple is type E1 that can measure the temperatures ranging of 0-700°C.

To test the granite specimens under elevated temperatures, the prepared specimens and loading platens are heated by heater coil, thermocouple and thermostat

for 24 hours before testing (Figure 1). A digital temperature regulator is used to maintain constant temperature to the specimen. The low temperature specimens are prepared by cooling them in a freezer for 24 hours. The changes of specimen temperatures between before and after testing are less than 5 K. As a result the specimen temperatures are assumed to be uniform and constant with time during the mechanical testing (i.e., isothermal condition). The axial and lateral loads monitored during the test are used to calculate the maximum, intermediate and minimum principal stresses (σ_1 , σ_2 and σ_3). They are the stresses along the three mutually perpendicular axes which will be used to derive the multi-axial strength criterion to be described later.

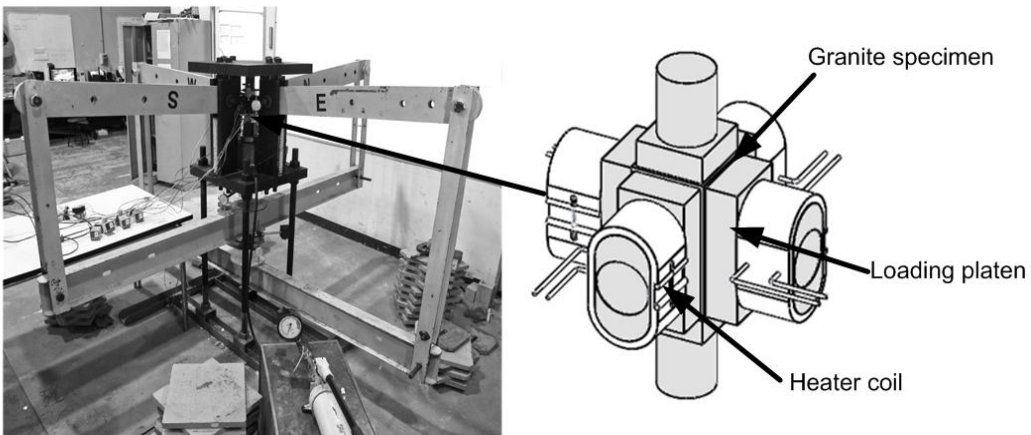


Figure 1. Polyaxial load frame used in the compressive strength testing of granite specimens with heater coil, thermocouple and thermostat.

4. Test Results

Post-test observations indicate that under low confining pressure, the specimens fail by the extension failure mode. Under the high confining pressure shear failure mode is observed. Figure 2 shows

stress-strain curves monitored from some granite specimens under various temperatures and confining pressures. For all specimens the two measured lateral strains induced by the same magnitude of the applied lateral stresses are similar. Some discrepancies may be due to the intrinsic variability of the

granite. The diagrams shown in Figure 2 indicate that both temperature and confining pressure can affect the granite strengths. Even through the specimens are tested under the same temperature, the specimen under higher confining stresses (σ_2, σ_3) fails under greater maximum principal stresses (σ_1).

The results indicate that under the same confining pressure the maximum principal stress at failure ($\sigma_{1,f}$) of granite decreases non-linearly with increasing temperature (T). This may be due to the fact that the thermal energy imposed onto the granite during the test can weaken the mineral compositions and their crystal interfaces, and hence making the rock softer. This behavior can be represented best by an empirical equation (Figure 3 and Table 1):

$$\sigma_{1,f} = \kappa \times (\exp(\beta/T) + (\alpha \times \sigma_3)) \quad (1)$$

The parameters κ , β , and α are empirical parameters. A good correlation is obtained between the test results and the proposed criterion ($R^2 = 0.996$).

To incorporate the intermediate principal stress (σ_2) the test results can be

presented in terms of the octahedral shear stress at failure ($\tau_{oct,f}$) as a function of mean stress (σ_m), as shown in Figure 4 and Table 1, where (15):

$$\tau_{oct,f} = \{1/3[(\sigma_1-\sigma_2)^2 + (\sigma_2-\sigma_3)^2 + (\sigma_3-\sigma_1)^2]\}^{1/2} \quad (2)$$

$$\sigma_m = 1/3(\sigma_1 + \sigma_2 + \sigma_3) \quad (3)$$

The diagram in Figure 4 clearly indicates that the effect of temperature on the granite strength is larger when the granite is under higher confining pressures. Linear relations can be observed at all temperature levels, and can be represented by

$$\tau_{oct,f} = \delta \times (\exp(\eta/T) + (\lambda \times \sigma_m)) \quad (4)$$

The parameters δ , η , and λ are empirical parameters. A good correlation is obtained between the test results and the proposed criterion. The coefficient of correlation (R) obtained from the regression analyses is equal to 0.999, indicating that the proposed equation fits very well to the test results.

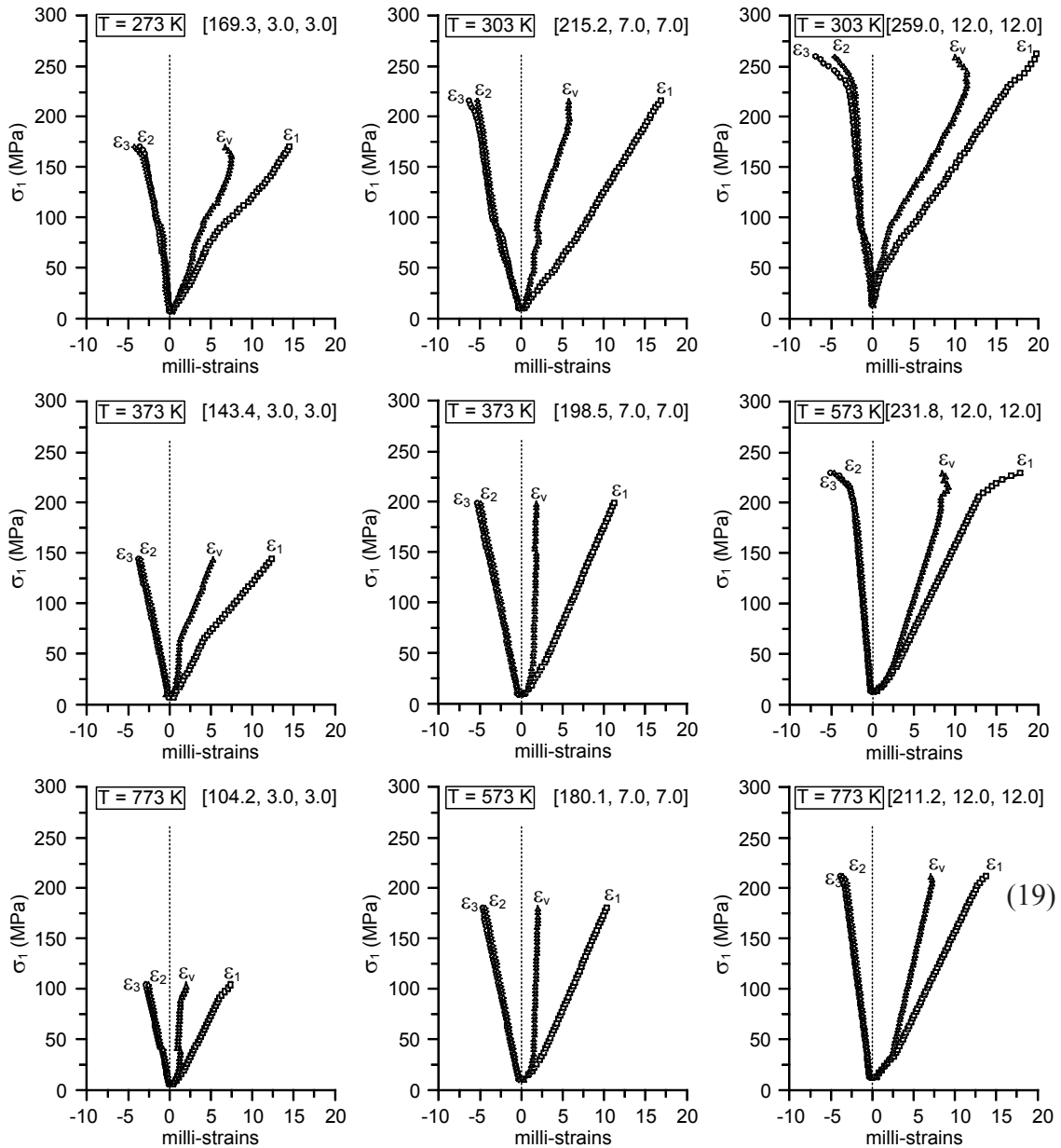


Figure 2. Stress-strain curves obtained from compression testing for some granite specimens with different temperatures. Numbers in brackets indicate $[\sigma_1, \sigma_2, \sigma_3]$ at failure.

(19)

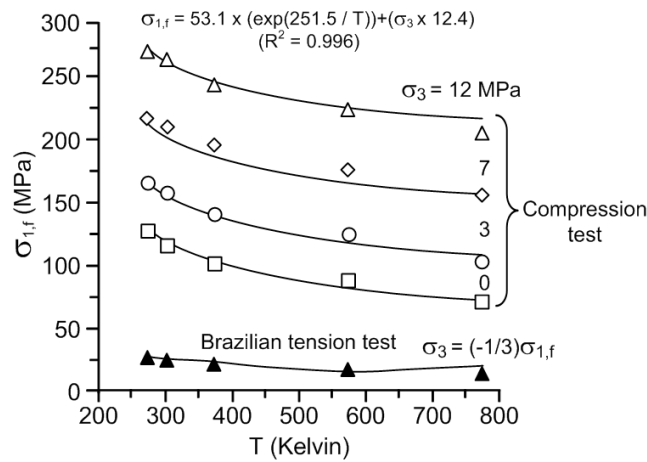


Figure 3. Major principal stresses at failure as a function of temperature.

Table 1. Strengths of granite.

| T (K) | σ ₃ (MPa) | σ ₁ (MPa) | σ _m (MPa) | τ _{oct,f} (MPa) |
|-------|----------------------|----------------------|----------------------|--------------------------|
| 273 K | -8.57 | 25.8 | 2.86 | 16.17 |
| | 0 | 131.1 | 43.67 | 61.79 |
| | 3 | 169.3 | 58.67 | 78.37 |
| | 7 | 222.2 | 78.67 | 101.45 |
| | 12 | 277.8 | 100.33 | 125.28 |
| 303 K | -7.79 | 23.37 | 2.59 | 14.69 |
| | 0 | 118.8 | 39.67 | 56.01 |
| | 3 | 161.1 | 55.67 | 74.54 |
| | 7 | 215.2 | 76.33 | 98.12 |
| | 12 | 269.2 | 98.00 | 120.00 |
| 373 K | -6.58 | 19.74 | 2.19 | 12.41 |
| | 0 | 104.1 | 34.67 | 49.06 |
| | 3 | 143.4 | 50.00 | 66.18 |
| | 7 | 198.5 | 71.33 | 90.28 |
| | 12 | 250.6 | 91.00 | 112.49 |
| 573 K | -5.43 | 16.29 | 1.81 | 10.24 |
| | 0 | 90.4 | 30.00 | 42.63 |
| | 3 | 127.7 | 44.33 | 58.77 |
| | 7 | 180.1 | 64.67 | 81.62 |
| | 12 | 231.8 | 84.33 | 102.04 |
| 773 K | -4.33 | 12.99 | 1.44 | 8.16 |
| | 0 | 73.1 | 24.33 | 39.00 |
| | 3 | 104.2 | 37.00 | 47.68 |
| | 7 | 157.9 | 57.67 | 71.14 |
| | 12 | 211.7 | 78.00 | 94.13 |

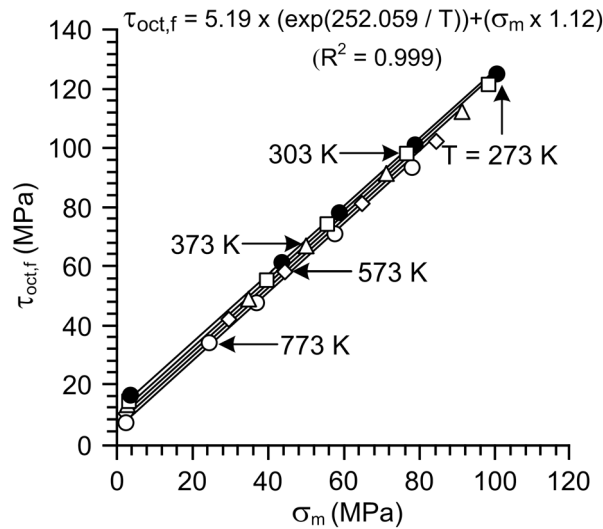


Figure 4. Octahedral shear strengths at failure of granite as a function of mean stress.

5. Hoek and Brown Criterion

The empirical relationship between the principal stresses associated with the failure of rock can be calculated from Hoek - Brown criterion given by equation (16):

$$\sigma_1 = \sigma_3 + (m\sigma_{c,HB}\sigma_3 + s\sigma_c^2)^{1/2} \tag{5}$$

where σ_1 is the major principal stress at failure,

σ_3 is the minor principal stress applied to the specimen,

$\sigma_{c,HB}$ is the uniaxial compressive strength of the intact rock material in the specimen, m and s are constants which depend upon the properties of the rock and upon the extent to which it has been broken before being subjected to the stresses σ_1 and σ_3 .

For intact rock, $s = 1$ and the uniaxial compressive strength $\sigma_{c,HB}$ and the material constant m are given by Hoek and Brown (16).

Regression analysis of equation (5) with the test data indicate that the parameter “ m ” increase with increasing temperature (Table 2). This can be explained by that as the temperature increases, the uniaxial compressive strength parameters in the Hoek and Brown criterion ($\sigma_{c,HB}$) decrease. This agrees reasonably well with the test results as shown in Figure 3 (for $\sigma_3 = 0$) and Table 1 (at $\sigma_3 = 0$).

The shear stress (τ) and normal stress (σ_n) can be calculated from the Mohr envelope given by (16):

$$\sigma_n = \sigma_3 + (\tau_m^2 / (\tau_m + ((m \times \sigma_{c,HB}) / 8))) \tag{6}$$

$$\tau = (\sigma_n - \sigma_3) \times (1 + ((m \times \sigma_{c,HB}) / (4 \times \tau_m)))^{1/2} \tag{7}$$

where $\tau_m = 1/2(\sigma_1 - \sigma_3)$. Results for the σ_n , τ , m , and $\sigma_{c,HB}$ are summarized in Table 2. In this case, since the rock specimens are intact, parameter s equals 1.0.

The cohesion (c) and internal friction angle (ϕ) can be determined from the

strength results for each temperature level using the following relations (16):

$$\tan \phi_i = A \times B \left(\left(\frac{\sigma_n}{\sigma_c} \right) - \left(\frac{\sigma_t}{\sigma_{c,HB}} \right) \right)^{B-1} \quad (8)$$

$$c_i = \tau - \sigma_n \tan \phi_i \quad (9)$$

The values of the constants A and B can be determined by linear regression

analysis. They are determined from the τ - σ_n curves at $\sigma_n = 20$ MPa. It is found that the cohesion decreases non-linearly while friction angle decreases linearly with increasing temperature.

$$c = 450.29 \times T^{-0.57} \quad (10)$$

$$\phi = -0.001 \times T + 58.70 \quad (11)$$

Table 2. Shear stress and normal stress at failure.

| T (K) | σ_3 (MPa) | $\sigma_{c,HB}$ (MPa) | m | R ² | τ (MPa) | σ_n (MPa) |
|----------|---------------------|--------------------------|-------|----------------|-----------------|---------------------|
| 273 | -8.57 | 153.40 | 21.86 | 0.945 | 60.27 | 25.73 |
| | 0 | | | | 229.04 | 131.00 |
| | 3 | | | | 291.56 | 170.00 |
| | 7 | | | | 374.92 | 222.00 |
| | 12 | | | | 463.09 | 277.00 |
| 303 | -7.79 | 143.15 | 23.34 | 0.943 | 55.36 | 23.37 |
| | 0 | | | | 211.61 | 119.00 |
| | 3 | | | | 280.24 | 161.00 |
| | 7 | | | | 368.47 | 215.00 |
| | 12 | | | | 458.33 | 270.00 |
| 373 | -6.58 | 124.61 | 24.55 | 0.954 | 46.99 | 19.74 |
| | 0 | | | | 181.94 | 104.00 |
| | 3 | | | | 246.01 | 144.00 |
| | 7 | | | | 335.70 | 200.00 |
| | 12 | | | | 414.18 | 249.00 |
| 573 | -5.43 | 105.46 | 25.96 | 0.962 | 38.95 | 16.29 |
| | 0 | | | | 154.12 | 90.00 |
| | 3 | | | | 211.93 | 127.00 |
| | 7 | | | | 294.73 | 180.00 |
| | 12 | | | | 371.29 | 229.00 |
| 773 | -4.33 | 84.06 | 28.95 | 0.957 | 30.28 | 12.99 |
| | 0 | | | | 120.69 | 73.00 |
| | 3 | | | | 168.90 | 105.00 |
| | 7 | | | | 250.26 | 159.00 |
| | 12 | | | | 327.09 | 210.00 |

6. Coulomb Criterion

Based on the Coulomb criterion the cohesion (c) and internal friction angle (ϕ) can be determined from the strength results for each temperature using the following relation (15):

$$\sigma_1 = \sigma_c + \sigma_3 \tan^2 [(\pi/4) + (\phi/2)] \quad (12)$$

$$\sigma_c = 2c \tan [(\pi/4) + (\phi/2)] \quad (13)$$

The cohesion and friction angle vary with temperature which are similar to those obtained by using the Hoek and Brown criterion.

$$c = 455.69 \times T^{-0.57} \quad (14)$$

$$\phi = -0.0011 \times T + 58.17 \quad (15)$$

Note that the friction angle (ϕ) and cohesion (c) equations obtained from the Hoek and Brown criterion are slightly different from those from the Coulomb criterion. This is due to the fact that the Hoek and Brown criterion is in non-linear form (square-root) while the Coulomb criterion is a linear function.

7. Elastic Parameters

The elastic modulus (E) and Poisson's ratio (ν) are determined from the tangent of the stress-strain curves at 50% failure stress. The elastic modulus (E), Poisson's ratio (ν), shear modulus (G) and bulk modulus (K) can be determined for each specimen using the following relations:

$$G = (1/2) (\tau_{oct} / \gamma_{oct}) \quad (16)$$

$$\lambda = (1/3) [(3\sigma_m / \Delta) - 2G] \quad (17)$$

$$E = 2G (1 + \nu) \quad (18)$$

$$\nu = \frac{\lambda}{2(\lambda + G)} \quad (19)$$

$$K = \frac{E}{3(1 - (2\nu))} \quad (20)$$

where Δ is volumetric strain which can be calculated from the summation of the major, intermediate and minor principal strains ($\epsilon_1 + \epsilon_2 + \epsilon_3$) measured during the test.

Nonlinear variations of these parameters with respect to temperature are observed from the results, as shown in Figure 5. Good correlations are obtained when they are fitted with the following linear equations:

$$E = 68.11 \cdot T^{-0.28} \quad (21)$$

$$G = 26.09 \cdot T^{-0.28} \quad (22)$$

$$K = 57.07 \cdot T^{-0.29} \quad (23)$$

$$\nu = (-6 \cdot 10^{-6}) \cdot T + 0.29 \quad (24)$$

The results indicate that the elastic, shear, and bulk moduli decrease with increasing temperature. They tend to be independent of the confining pressure, as suggested by the small standard deviations indicated on the diagrams in Figure 5. The Poisson's ratios tend to be independent of the temperature and confining pressure.

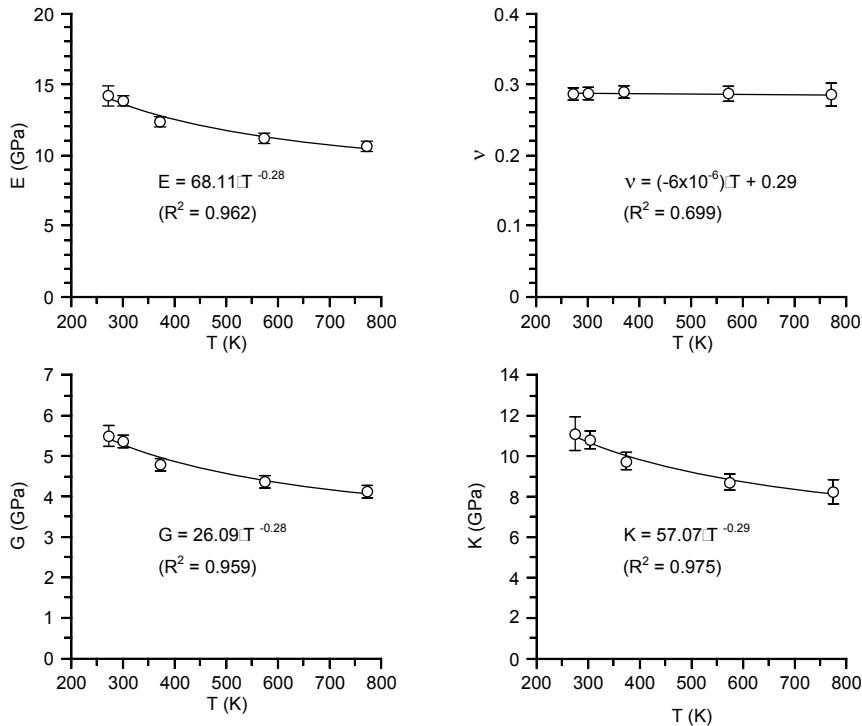


Figure 5. Elastic parameters of granite as a function of temperature.

8. Strain Energy Density Criterion

The strain energy density principle is applied here to describe the rock strength and deformation under different temperatures. Assuming that for each temperature level the granite is linearly elastic prior to failure, the distortional strain energy (W_d) and the mean strain energy (W_m) as failure can be determined for each specimen using the following relations (17):

$$w_d = \frac{3}{4}(\tau_{oct}^2 / G) \tag{25}$$

$$w_m = \sigma_m^2 / 2K \tag{26}$$

The elastic parameters G and K can be defined as a function of the testing temperature, and hence the granite strengths from different temperatures can be correlated. By substituting equations (22) into (25) and

(23) into (26) the W_d at failure can therefore incorporate the effect of specimen temperature into the strength calculation.

The distortional strain energy for each granite specimen at failure, that implicitly takes the temperature effect into consideration, is plotted as a function of the mean strain energy in Figure 6. The data can be described best by a linear equation:

$$W_d = A_{Th} \cdot W_m + B_{Th} \tag{27}$$

The parameters A_{Th} and B_{Th} are empirical constants depending on the strength and thermal response of the rock. For the Tak granite $A_{Th} = 4.49$ and $B_{Th} = 0.09$ MPa. A good correlation is obtained between the test results and the proposed criterion ($R^2 = 0.992$).

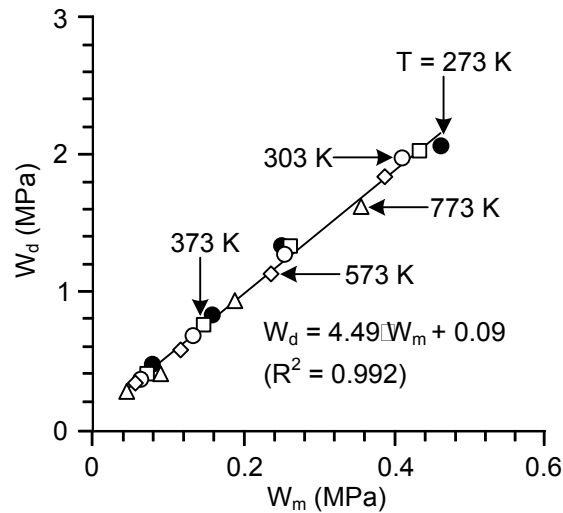


Figure 6. Distortional strain energy as a function of mean strain energy.

9. Discussions and Conclusion

This study experimentally determines the granite strengths under different constant temperatures separately. For each temperature level the testing is assumed to be under isothermal condition (constant temperature with time during loading). For this simplified approach the granite specimens subject to different temperatures have been taken as different materials. As a result the induced thermal stress or thermal energy imposed on the granite specimens has not been explicitly incorporated into the initial strength calculation. This approach is different from the conventional thermo-mechanical analysis.

The decrease of the granite strength as the temperature increases suggest that the applied thermal energy before the mechanical testing makes the granite weaker, and more plastic – failing at lower stress and higher strain with lower elastic and shear modulus. The temperature effect is larger when granite is under higher mean stress. In order to

consider the temperature dependency of the failure stress and strain and elastic properties the strain energy density concept is applied. Assuming that the granite is non-linearly elastic before failure, the distortional strain energy (W_d) at failure can be calculated as a function of mean strain energy (W_m). In Figure 6 at a given W_m the W_d decreases with increasing temperature. The differences of W_d from one temperature to the other therefore correspond to the difference of thermal energy imposed on the specimens.

The single multi-axial strength criterion (27) for granite under various confining pressures and temperatures implicitly considers the effect of the thermal energy by incorporating the empirical equations between the elastic parameters and temperature into the W_d – W_m relation (Figure 6). The strain energy criterion agrees well with the strength results from different temperature levels. Since the analysis is intended to determine the short-term strength, the long-term deformations induced by the mechanical and thermal loadings are not considered here.

10. Acknowledgements

This study is funded by Suranaree University of Technology and by the Higher Education Promotion and National Research University of Thailand. Permission to publish this paper is gratefully acknowledged.

12. References

- (1) Vosteen H, Schellschmidt R. Influence of temperature on thermal conductivity, thermal capacity and thermal diffusivity for different types of rock. *Phys. Chem. Earth.* 2003;28(9-11):499-509.
- (2) Shimada M, Liu J. Temperature dependence of strength of rock under high confining pressure, *Annals Disas. Prev. Res. Inst.* 2000;43B-1:75-84.
- (3) Xu X, Gao F, Shen XM, Xie HP. Mechanical characteristics and microcosmic mechanisms of granite under temperature loads. *J China Univ Mining and Technol.* 2008;18(3):413-417.
- (4) Bergman MS. Nuclear waste disposal. *Subsurf Space.* 1980;2:791-1005.
- (5) US Department of Energy. Statement of the position of the United States Department of Energy in the matter of rulemaking on the storage and disposal of nuclear wastes, Report DOE/NE-0007; 1980.
- (6) Logan SE. Deep self-burial of radioactive wastes by rock melting capsules. *Trans. Am. Nucl. Soc. Ann. Mtg.* 1973;21:111-124.
- (7) Heuze FE. On the geotechnical modelling of high-level nuclear waste disposal by rock melting. Lawrence Livermore National Laboratory Report UCRL-53183; 1981.
- (8) Etienne FH, Houpert R. Thermally induced microcracking in granites: characterization and analysis. *Int. J. Rock. Mech. Min. Sci. Geomech.* 1989;26(2):125-134.
- (9) Dwivedi RD, Goel RK, Prasad VVR, Amalendu S. Thermo-mechanical properties of Indian and other granites. *Int. J. Rock. Mech. Min. Sci.* 2008;45(3):303-315.
- (10) Mahawat C, Atherton MP, Brotherton MS. The Tak Batholith, Thailand: the evolution of contrasting granite types and implications for tectonic setting. *J. Southeast Asian Earth Sci.* 1990;4(1):11-27.
- (11) ASTM D 4543-85. Standard test method for preparing rock core specimens and determining dimensional and shape tolerances. *Annual Book of ASTM Standards.* Vol. 04.08. Philadelphia.
- (12) ASTM D 3967-95. Standard test method for splitting tensile strength of intact rock core specimens. *Annual Book of ASTM Standards.* Vol. 04.08. Philadelphia.
- (13) Fuenkajorn K, Kenkhunthod N. Influence of loading rate on deformability and strength of three Thai sandstones. *Eng. Geol.* 2010;28: 707-715.

- (14) ASTM D3967-08. Standard test method for splitting tensile strength of intact rock core specimens. ASTM Annual Book of Standards. Vol. 04.08. West Conshohocken.
- (15) Jaeger JC, Cook NGW, Zimmerman RW. Fundamentals of rock mechanics. 4th ed. Blackwell Publishing: Oxford; 2007.
- (16) Hoek E, Brown ET. Underground excavations in rock, The Institution of Mining and Metallurgy, Portland Place: London; 1980.
- (17) Fuenkajorn K, Phueakphum D. Effects of cyclic loading on mechanical properties of Maha Sarakham salt. Eng. Geol. 2010;112:43-52.P